

CEAS Technical Report No. 682

**Personal Communication Systems Using
Multiple Hierarchical Cellular Overlays**

Lon-Rong Hu and Stephen S. Rappaport
Department of Electrical Engineering

State University of New York at Stony Brook
College of Engineering and Applied Sciences
Stony Brook, New York 11794
February, 1994

Personal Communication Systems Using Multiple Hierarchical Cellular Overlays

Lon-Rong Hu and Stephen S. Rappaport

Department of Electrical Engineering
State University of New York
Stony Brook, NY 11794-2350

phone: (516) 632-8394 / 632-8400
fax: (516) 632-8494
e-mail: rappaport@sbee.sunysb.edu

Abstract

A personal communication system with multiple hierarchical cellular overlays is considered. The system can include a *terrestrial segment* and a *space segment*. The *terrestrial segment*, consisting of *microcells and macrocells*, provides high channel capacity by covering service areas with microcells. Overlaying macrocells cover spots that are difficult in radio propagation for microcells and provide overflow groups of channels for clusters of microcells. At the highest hierarchical level, communications satellites comprise a *space segment*. The satellite beams overlay clusters of terrestrial macrocells and provide primary access for satellite-only subscribers. Call attempts from cellular/satellite dual subscribers are first directed to the terrestrial cellular network, with satellites providing necessary overlay. At each level of the hierarchy, hand-off calls are given priority access to the channels.

The mathematical structure is that of a multi-layer hierarchical overflow system. An analytical model for teletraffic performance (including hand-off) is developed. Theoretical performance measures are calculated for users having different mobility characteristics. These show the carried traffic, traffic distribution, blocking, and forced termination probabilities.

I Introduction

As mobile teletraffic demands increase dramatically, interest in cellular system structure with *hierarchical macrocell overlays* has emerged [1]. Recently, the development of universal personal communication systems (PCS) has motivated the use of satellites for large seamless coverage. Satellite constellations have been proposed for low earth orbit (LEO) [2] or medium earth orbit (MEO) [3]. Some technical issues behind the choice of non-geostationary earth orbit (GEO) for PCS satellite constellations are transmission delay, path loss, and the antenna sizes required to produce narrow beams (i.e. small cells). A number of satellite-based PCS are actively underway and expected to be in full service by the year of 2000. In the future microcellular environment, the use of satellites and integration of terrestrial cellular and satellite-based PCS is anticipated [4].

The advent of satellite-based PCS introduces a new dimension to terrestrial cellular communications. *Without satellite participation*, terrestrial cellular systems would be primarily restricted to regional service. *With satellites alone*, high channel capacity can only be achieved by employing a large number of narrow beams; each spot beam forms the coverage area of a small cell. A narrow spot beam can only be generated by a *very large antenna aperture* and the resultant system will suffer *frequent hand-offs* between different beams (cells) during operation. It is thus evident that if a PCS is to have seamless radio coverage and sufficient capacity to accommodate anticipated high teletraffic, *integration of satellite network and terrestrial cellular system may be desirable*.

In this chapter, a space/terrestrial personal communication system with multiple hierarchical cellular overlays is considered. The *terrestrial segment* consists of *microcells and macrocells*. Service areas are covered by microcells while overlaying macrocells cover spots that are difficult in radio propagation for microcells and provide overflow groups of channels for clusters of microcells. At the highest hierarchical level, communications satellite beams overlay clusters of terrestrial macrocells in addition to providing primary access for satellite-only subscribers. For cellular/satellite dual subscribers, call attempts are first directed to a terrestrial cellular network, with satellites providing necessary overlay. The access methods (frequency division multiple access (FDMA), time division multiple access (TDMA), and code division multiple access (CDMA)) used at different hierarchical levels of the system need not be the same. At each level of the hierarchy, hand-off calls are given priority access to channels. Thus, the entire system provides high system capacity, wide coverage areas, and inherent load-balancing capability. Related work includes: [5], which considers introducing

overlying macrocell to reduce the forced termination of calls in progress in microcellular personal communication networks; [6]-[7], which consider the multiple access options for the support of personal communication systems with hierarchical cell structure. Additional work dealing with hierarchical cellular systems appears in [8].

The mathematical structure of the system described here is that of a multi-layer hierarchical overflow system. An *exhaustive (global)* state description used in [1] to allow consideration of hand-off traffic is not practical in the context of multi-layer overlay because of the large number of states needed for computational purposes. As an alternative, an analytical method using both state descriptions and *Interrupted Poisson Process* [9] is developed. Throughout the analysis, our model remains within the framework of a birth-death process. In this chapter, theoretical performance characteristics for users having different mobilities are calculated and presented. These show the carried traffic, traffic distribution, blocking, and forced termination probabilities.

II System Description

Figure 1 depicts a large geographical region tessellated by hexagonal cells, referred to as *microcells*. Every N_1 microcells are overlaid by a larger cell, called a *macrocell*. Every N_2 macrocells are in turn overlaid by a satellite beam, called a *spot beam*. The numbers N_1 and N_2 are chosen for example purposes as 7 throughout this chapter. Gateways serving each cell are linked to the fixed terrestrial network, in which *call routing* and *call hand-off* are carried out.

The region is traversed randomly by a large number of mobile platforms. Mobile platforms are classified into *high* and *low mobility* platforms. Users are classified into *satellite-only* and *dual (cellular/satellite)* users in terms of the service subscribed. Each microcell, macrocell, and spot beam is allocated a number of channels, C_1 , C_2 , and C_3 , respectively, of which C_{hi} , ($i = 1, 2, 3$) channels are reserved for the exclusive use of hand-off calls. New call originations that are initially directed to *spot beams*, called *primary new calls*, can access C_s more *spot beam* channels than overflowed new calls. For the system based on non-GEO, hand-off may occur due to the *motion of user platforms* or due to the *motion of satellites*. Since the focus here is on the assignment and availability of communication resources, the term *hand-off* here exclusively means the event of reallocating radio channels while a call is in progress *due to the motion of user platforms*.

We consider the system operation as follows:

- (a) For any new call and hand-off request originated from a *dual* user there is *one cell at each* hierarchical level that is *preferred*. A *preferred cell of level- i* is the cell of level i that receives strongest signal power in comparison with other cells of the same level.
- (b) A new call origination from a *dual user* is directed to *the lowest* level of system hierarchy that can provide a radio link with satisfactory quality. Taking the condition of radio propagation into account, a new call origination from a dual user is directed to the preferred microcell immediately with probability f_1 , to the preferred macrocell with f_2 , and to the preferred spot beam with f_3 . If directed to a preferred microcell immediately and the number of channels in use in the preferred microcell is equal to or greater than $C_1 - C_{h1}$, this new call is overflowed to its *preferred macrocell*. If the number of channels in use in the preferred macrocell is again equal to or greater than $C_2 - C_{h2}$, the call is overflowed to its *preferred spot beam cell*. Overflowed new calls, however, can only access $C_3 - C_{h3} - C_s$ channels out of C_3 allocated channels of a spot beam. New call originations *from satellite-only users and those from dual users but are initially directed to a preferred spot beam* will be accommodated if the number of channels in use in the spot beam is less than $C_3 - C_{h3}$; otherwise, it is blocked and cleared from the system. The first available idle channel will be seized by a call until the call is satisfactorily completed or the communicating platform leaves the communication range of its current gateway.
- (c) A hand-off request will be initiated *only if* a communicating platform leaves the communication range of its *current gateway*.
- (d) A call that initiates a hand-off request always searches for idle channels starting from a preferred cell that has the *same hierarchical level* as the source cell.
- (e) For the sake of mathematical tractability, we consider that once a call is served at certain hierarchical level, it will continue service at the same or a higher level but *not revert* to service at a lower level.

Note that since the direction of hand-off overflow is upward-only in system hierarchy, rule (d), and a call will not revert to service at lower level, rule (e), the system operation tends to create a traffic distribution in which high mobility platforms are more likely to be served by the larger cells, i.e. cells that are higher in system hierarchy. This traffic distribution is achieved without any other mechanism for mobility management, such as those based on speed measurements for initial cell assignment.

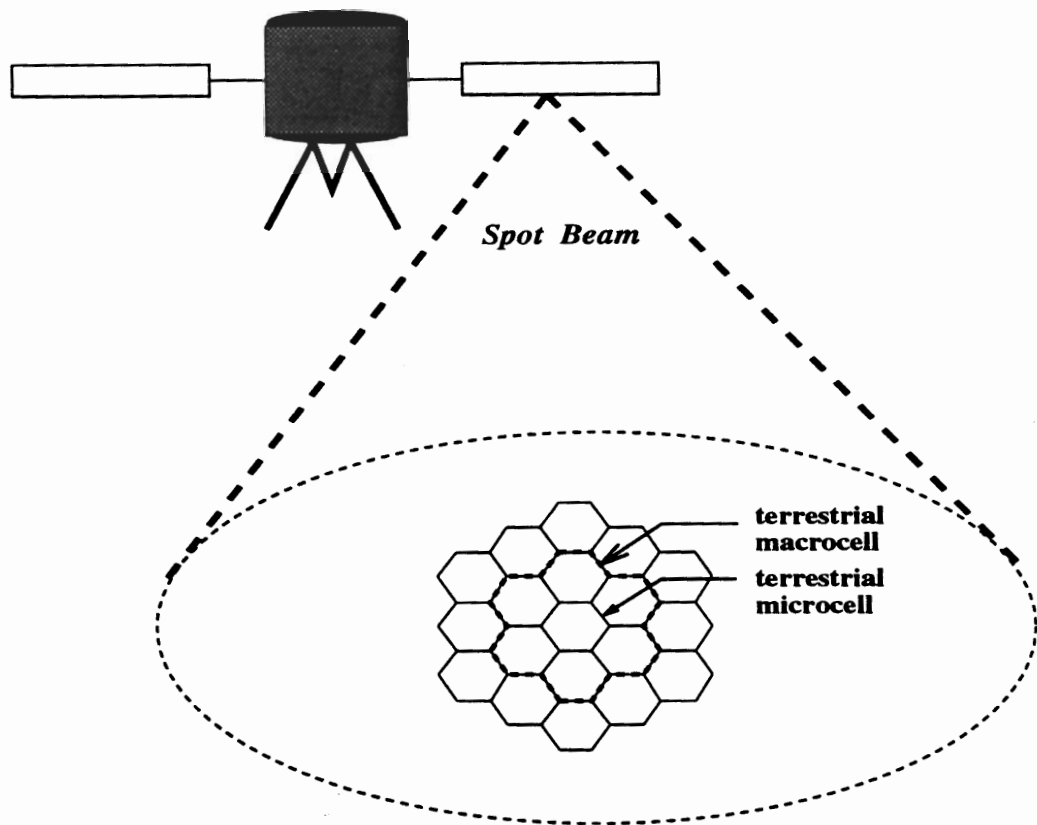


Figure 1: The architecture of a multi-layer hierarchically overlaid system.

III Mathematical Preliminaries

III.1 Approach

In the homogeneous case, all cells of the same hierarchical level are statistically identical. We can analyze the overall system by focusing on only one given cell in each level, and consider the statistical behavior of this focused cell under the conditions that its neighboring cells exhibit their typical random behavior *independently*.

The following memoryless assumptions allow the problem to be cast in the framework of multi-dimensional birth-death processes. Similar assumptions have served telecommunications traffic engineering well for many years.

(1) The *new call arrival* processes offered to a given cell at each system level are Poisson processes. The mean new call arrival rates to microcells, macrocells, and spot beams *from high mobility platforms* are Λ_{H1} , Λ_{H2} , and Λ_{H3} , respectively, and the mean new call arrival rates *from low mobility platforms* are Λ_{L1} , Λ_{L2} , and Λ_{L3} , respectively.

(2) The *hand-off call arrival* processes to a given cell at each level due to the motion of *high mobility platforms* are Poisson processes with mean hand-off arrival rates Λ_{Hh1} , Λ_{Hh2} , and Λ_{Hh3} , respectively. Similarly, Λ_{Lh1} , Λ_{Lh2} , and Λ_{Lh3} are the mean hand-off arrival rates resulting from *low mobility platforms*. These hand-off parameters are to be determined from the underlying processes that drive the system. In subsequent discussion we will explain how these rates are determined.

(3) The dwell time is the amount of time that a communicating platform remains *within communications range* of a given gateway. For *high mobility* communicating platforms in a cell of level i ($i = 1, 2, 3$), the dwell time is a random variable (R.V.), T_{HDi} , having the negative-exponential distribution (n.e.d.) with mean equal to U_{HDi}^{-1} . For *low mobility* communicating platforms, the dwell time is denoted as T_{LDi} ($i = 1, 2, 3$) with mean U_{LDi}^{-1} .

(4) The *unencumbered session duration* of a call is the amount of time that the call would remain in progress if it could continue to completion *without forced termination due to hand-off failure*. The unencumbered session duration, T , regardless of the *platform mobility or user class*, is a n.e.d. R.V. with mean equal to μ^{-1} .

III.2 Mathematical Structure

The mathematical structure of the multi-layer hierarchically overlaid system is that of a multi-layer hierarchical overflow system, in which microcells receive Poisson input streams,

whereas each overlaying cell (*macrocells* and *spot beams*) receives Poisson input streams in addition to non-Poisson overflow traffic components from subordinate cells. A schematic diagram showing the mathematical structure is depicted in Figure 2. The number of subordinate cells is 7 for each macrocell and spot beam, for simplicity, however, only the overflow components from one subordinate cell is shown.

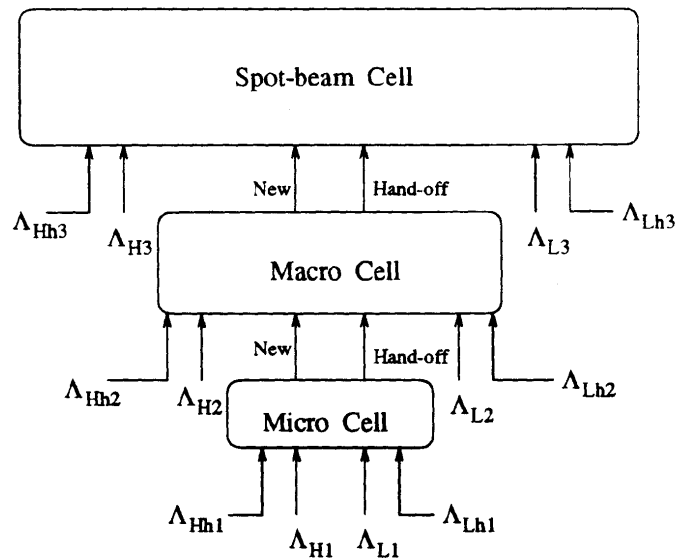


Figure 2: The mathematical structure of a multi-layer hierarchically overlaid system.

In Figure 2, a microcell receives *new call originations* from high- (Λ_{H1}) and low mobility platforms (Λ_{L1}), respectively. Λ_{Hh1} and Λ_{Lh1} are the average rates of hand-off call arrival processes resulting from high- and low mobility platforms, respectively. Calls that can not be served by this microcell are overflowed to its overlaying macrocell. A macrocell receives overflow streams from subordinate microcells, each of which consisting of new call and hand-off call components. Other components offered to a macrocell, Λ_{H2} , Λ_{L2} , Λ_{Hh2} , and Λ_{Lh2} have similar meanings as their counterparts in a microcell. Note that the overflowed new call stream and the overflowed hand-off stream have to be treated separately so that our cut-off priority scheme for hand-off calls can be at work. The spot beam level follow a similar line of explanation.

IV Mathematical Analysis

Clearly, two different types of traffic (arrival processes), *Poisson* and *overflow traffic*, must be considered. Analysis of a multi-layer hierarchically overlaid system starts from the lowest hierarchical level of the system and proceeds upward until the highest level is reached. Performance measures can then be derived.

IV.1 Microcell Level

A given microcell can be characterized at any instant as being in a state that is described by the number of communicating *high mobility* and *low mobility* platforms, denoted by h and l , respectively. Both platform types have identical *unencumbered session durations*, μ^{-1} , but are distinguished by different microcell *dwel times*; U_{HD1}^{-1} for high mobility and U_{LD1}^{-1} for low mobility platforms. The arrival streams to a given microcell are Poisson with rates Λ_{H1} , Λ_{L1} , Λ_{Hh1} , and Λ_{Lh1} . Of these, the mean hand-off arrival rates Λ_{Hh1} and Λ_{Lh1} must be determined from underlying processes. To formulate state equations, they are temporarily assumed to be given. We will subsequently address how to determine these parameters.

Let $P_1(h, l)$ be the statistical-equilibrium probability that there are h platforms of *high mobility* type and l platforms of *low mobility* type simultaneously in service in a given microcell. The number of channels allocated to a microcell is C_1 , of which C_{h1} channels are reserved for the exclusive use of hand-off calls. Because of hand-offs, state transitions of adjacent microcells are coupled. Similarly, state transitions of adjacent macrocells are coupled, as well as adjacent spot beam state transitions. Thus a complete characterization of the system would require use of a *system state* consisting of a concatenation of states of all cells at all levels. The dimensionality problem renders this approach unusable. The difficulty is circumvented using the basic notion described in [10] and [11]. Specifically, it is noted that any hand-off departure (of any given platform type) from a microcell corresponds to a hand-off arrival to another microcell. Thus, for a homogeneous system in statistical equilibrium, the average hand-off arrival rate (of any given platform type) to a microcell must equal the corresponding hand-off departure rate. This allows a decoupling of any microcell from its neighbors and permits an approximate analysis by consideration of the microcell and its overlaying macrocell and spot beam. A similar argument is made at each level of the hierarchy. If the hand-off arrival rates are known, state equations can be formulated in the usual way [12]. An example state-transition diagram for the case $C_1 = 4$ and $C_{h1} = 1$ is

shown in Figure 3. So beginning with an initial guess of hand-off arrival rates, the equations are solved for the state probabilities, which are then used to determine the average hand-off departure rates. An iterative approach is used to update the hand-off arrival rates in much the same way as described in [10] and [11]. An important difference here is that there is also overflow from one hierarchical level to the next. Specifically, we begin with a guess of a value for Λ_{Hh1} and Λ_{Lh1} , respectively, and the complete calculation of state probabilities, $P_1(h, l)$, is performed. Revised values for Λ_{Hh1} and Λ_{Lh1} can be obtained using following expressions.

$$\begin{aligned}\Delta_{Hh1} &= \sum_{h=0}^{C_1} \sum_{l=0}^{C_1} h \cdot U_{HD1} \cdot P_1(h, l) \\ \Delta_{Lh1} &= \sum_{h=0}^{C_1} \sum_{l=0}^{C_1} l \cdot U_{LD1} \cdot P_1(h, l)\end{aligned}\quad (1)$$

The entire calculation is repeated until we find hand-off arrival rates, Λ_{Hh1} and Λ_{Lh1} , which result in equal hand-off departure rates, Δ_{Hh1} and Δ_{Lh1} , respectively. The resulting state probabilities and rates obtained, Λ_{Hh1} and Λ_{Lh1} , are the desired statistical equilibrium solution. The probability that a new call is denied access to a microcell channel and overflowed to its overlaying macrocell, denoted as P_{N1} , is written as

$$P_{N1} = \sum_{(h+l)=C_1-C_{h1}}^{C_1} P_1(h, l) , \quad (2)$$

and the probability that a hand-off call is overflowed to overlaying macrocell is

$$P_{h1} = \sum_{(h+l)=C_1} P_1(h, l) . \quad (3)$$

IV.2 Calculate Moments of Overflow Traffic

It has been shown in [13] that overflow traffic has a ‘peaked’ character and *the principal fluctuation characteristics of overflow type of non-random traffic are well characterized by their mean α and variance v* . Formulas to determine the n_{th} factorial moments of overflow traffic, $M_{(n)}$, for the case that A erlangs of Poisson traffic being offered to a set of S full-access primary channels was given by Kosten in 1937 [13]. The mean and variance of overflow traffic can be easily derived from factorial moments. For the system under discussion, however, Kosten’s formula is not directly applicable for two reasons. One is that the priority access for hand-off calls, render our system *not full-access for new calls*. Another is due to the

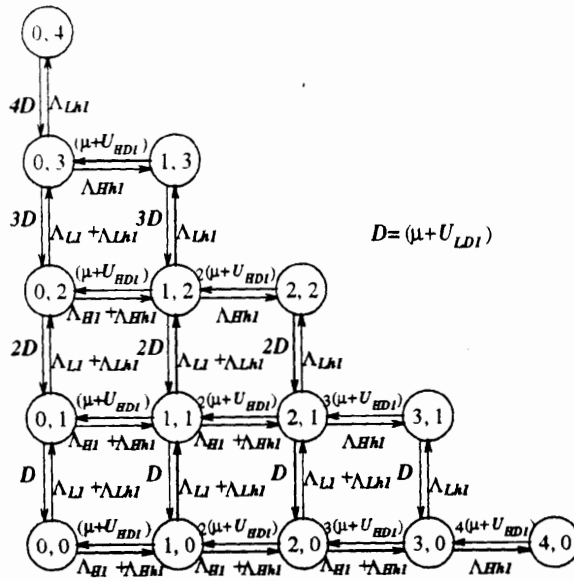


Figure 3: An example state-transition diagram for the analysis of a microcell whose $C_1 = 4$ and $C_{h1} = 1$.

presence of hand-off traffic. Kosten's formulas assume that the calls offered to the primary group *have no mobility*, a typical scenario in telephone engineering but not applicable in microcellular PCS context. As a result, a suitable mechanism to determine the moments of overflow traffic when hand-off traffic and cut-off priority are present in the primary group is essential.

We calculate the mean and variance of the traffic that overflow a subordinate microcell by introducing a *fictitious, infinite-server* overflow group as shown in Figure 4. The new call streams offered to a microcell, Λ_{H1} and Λ_{L1} , are given and the hand-off streams, Λ_{Hh1} and Λ_{Lh1} , were determined from previous microcell-level analysis. The fictitious infinite-server overflow group is to *catch* any call that overflows the primary group (a microcell). Thus the distribution of busy channels in the infinite-server overflow group is the distribution of calls overflowing a microcell. By choosing the number of channels in the fictitious overflow group, *Max*, sufficiently large when compared with the load submitted to a microcell, an "*overflowed calls held*" situation or infinite-server results can be approached as closely as desired. We found that no significant changes in calculated overflow moments are discernable if *Max* is taken to be three or more times the offered load.

The system of Figure 4 is described by a state (h, l, N) with equilibrium probability

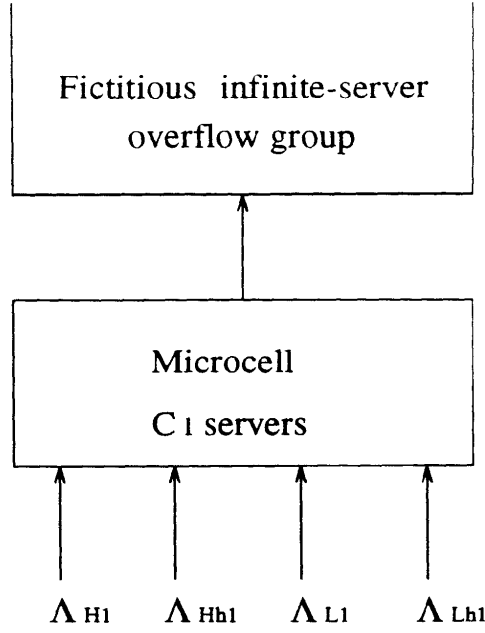


Figure 4: The calculation of traffic distribution that overflow a microcell.

$Q_1(h, l, N)$, in which h and l were defined earlier and N is the number of calls present on the (infinite-server) fictitious overflow group. Note that the calls served in a microcell have mobility as they were, but the calls served by the fictitious group, however, is *stationary*. State equations can be formulated and solved for the state probabilities in the usual way.

When the number of channels in use in a microcell is less than $C_1 - C_{h1}$, both new calls and hand-off calls will be accommodated in microcell regardless of the channel usage in the overlaying macrocell. Thus, the equilibrium state equations for the probabilities $\{Q_1(h, l, N)\}$ when $0 \leq (h + l) < (C_1 - C_{h1})$ and $0 \leq N \leq Max$ are given by

$$\begin{aligned}
& (\Lambda_{H1} + \Lambda_{L1} + \Lambda_{Hh1} + \Lambda_{Lh1} + (h + l + N)\mu + hU_{HD1} + lU_{LD1})Q_1(h, l, N) \\
& = (\Lambda_{H1} + \Lambda_{Hh1})Q_1(h - 1, l, N) + (\Lambda_{L1} + \Lambda_{Lh1})Q_1(h, l - 1, N) \\
& \quad + [(h + 1)\mu + (h + 1)U_{HD1}]Q_1(h + 1, l, N) \\
& \quad + [(l + 1)\mu + (l + 1)U_{LD1}]Q_1(h, l + 1, N) + (N + 1)\mu Q_1(h, l, N + 1) \\
& \quad [Q_1(-1, l, N) = Q_1(h, -1, N) = Q_1(h, l, Max + 1) = 0]
\end{aligned} \tag{4}$$

When $(C_1 - C_{h1}) \leq (h + l) < C_1$, new call arrivals will be overflowed to next higher hierarchy

for service while hand-off call are still accommodated by microcells. Specifically, let

$$\phi_{n'} = \begin{cases} 0 & \text{if } N = Max. \\ 1 & \text{otherwise.} \end{cases} \quad (5)$$

Then the state equations for $(h + l) = (C_1 - C_{h1})$, $(0 \leq N \leq Max)$, are

$$\begin{aligned} & (\Lambda_{H1}\phi_{n'} + \Lambda_{L1}\phi_{n'} + \Lambda_{Hh1} + \Lambda_{Lh1} + (h + l + N)\mu + hU_{HD1} + lU_{LD1})Q_1(h, l, N) \\ & = (\Lambda_{H1} + \Lambda_{Hh1})Q_1(h - 1, l, N) + (\Lambda_{L1} + \Lambda_{Lh1})Q_1(h, l - 1, N) \\ & \quad + (\Lambda_{H1} + \Lambda_{L1})Q_1(h, l, N - 1) + [(h + 1)\mu + (h + 1)U_{HD1}]Q_1(h + 1, l, N) \\ & \quad + [(l + 1)\mu + (l + 1)U_{LD1}]Q_1(h, l + 1, N) + (N + 1)\mu Q_1(h, l, N + 1) \\ & \quad [Q_1(h, l, -1) = Q_1(h, l, Max + 1) = 0] \end{aligned} \quad (6)$$

and equations for $(C_1 - C_{h1}) < (h + l) < C_1$, $(0 \leq N \leq Max)$, are written as

$$\begin{aligned} & (\Lambda_{H1}\phi_{n'} + \Lambda_{L1}\phi_{n'} + \Lambda_{Hh1} + \Lambda_{Lh1} + (h + l + N)\mu + hU_{HD1} + lU_{LD1})Q_1(h, l, N) \\ & = \Lambda_{Hh1}Q_1(h - 1, l, N) + \Lambda_{Lh1}Q_1(h, l - 1, N) + (\Lambda_{H1} + \Lambda_{L1})Q_1(h, l, N - 1) \\ & \quad + [(h + 1)\mu + (h + 1)U_{HD1}]Q_1(h + 1, l, N) \\ & \quad + [(l + 1)\mu + (l + 1)U_{LD1}]Q_1(h, l + 1, N) + [(N + 1)\mu]Q_1(h, l, N + 1) \\ & \quad [Q_1(h, l, -1) = Q_1(h, l, Max + 1) = 0] \end{aligned} \quad (7)$$

Finally, the equilibrium equations for boundary states $(h + l) = C_1$, $(0 \leq N \leq Max)$, are given by

$$\begin{aligned} & [(\Lambda_{H1} + \Lambda_{L1} + \Lambda_{Hh1} + \Lambda_{Lh1})\phi_{n'} + (h + l + N)\mu + hU_{HD1} + lU_{LD1}]Q_1(h, l, N) \\ & = (\Lambda_{H1} + \Lambda_{L1} + \Lambda_{Hh1} + \Lambda_{Lh1})Q_1(h, l, N - 1) + \Lambda_{Lh1}Q_1(h, l - 1, N) \\ & \quad + \Lambda_{Hh1}Q_1(h - 1, l, N) + [(N + 1)\mu]Q_1(h, l, N + 1) \\ & \quad [Q_1(h, l, -1) = Q_1(h, l, Max + 1) = 0] \end{aligned} \quad (8)$$

The system is completely described by Equations (4), (6), (7), (8), and the normalization equation

$$\sum_{h=0}^{C_1} \sum_{l=0}^{C_1} \sum_{N=0}^{Max} Q_1(h, l, N) = 1. \quad (9)$$

Once above state equations are solved, the mean and variance of the overflow distribution can be computed from state probabilities. Let α_i and v_i denote respectively the mean and

variance of the overflow distribution resulting from a subordinate microcell i . Then they can be obtained from the expressions

$$\alpha_i = \sum_{h=0}^{C_1} \sum_{l=0}^{C_1} \sum_{N=0}^{Max} N \cdot Q_1(h, l, N), \quad (10)$$

$$v_i = \left\{ \sum_{h=0}^{C_1} \sum_{l=0}^{C_1} \sum_{N=0}^{Max} N^2 \cdot Q_1(h, l, N) \right\} - \alpha_i^2. \quad (11)$$

IV.3 Overflow Traffic Modeling

The overflow stream seen by an overlaying macrocell is the aggregation of N_1 overflow streams, each of which results from a subordinate microcell. Let α_T and v_T represent respectively the *mean* and *variance* of the *composite overflow traffic* seen by an overlaying macrocell. Since microcells are *independent* each other, it follows that

$$\alpha_T = \sum_{i=1}^{N_1} \alpha_i \quad (12)$$

$$v_T = \sum_{i=1}^{N_1} v_i, \quad (13)$$

where α_i is the mean of overflow traffic from a subordinate microcell and N_1 is the number of microcells overlaid by a macrocell.

The approach to modeling overflow traffic is to identify a stochastic process that can generate the same mean and variance (or *moments* in general terms) and is simple for analysis. *As long as the moments of a stochastic process are sufficiently close to those of the overflow traffic, the stochastic properties of overflow distribution are accurately preserved.* In this chapter, the composite overflow stream is modeled by an *interrupted Poisson process (IPP)* [9]. An *IPP* is a two-state Markov-Modulated Poisson Process (MMPP) [14] in which a Poisson process is modulated by a random switch that is alternately turned on for an exponentially distributed time and turned off for another (independent) exponentially distributed time. Let λ be the intensity of modulated Poisson process, γ^{-1} be the mean on-time of the random switch, and ω^{-1} be the mean off-time of the random switch. Then given the mean and variance of an overflow traffic, three *IPP* parameters, λ , γ , and ω are to be chosen such that the same mean and variance will be generated. Figure 5 functionally depicts the conceptual structure of an *IPP* and its use for modeling overflow traffic.

To the problem at hand, we first use the *equivalent random method* [13] to determine an equivalent full-access group, S , associated with an equivalent random load, A , such that the

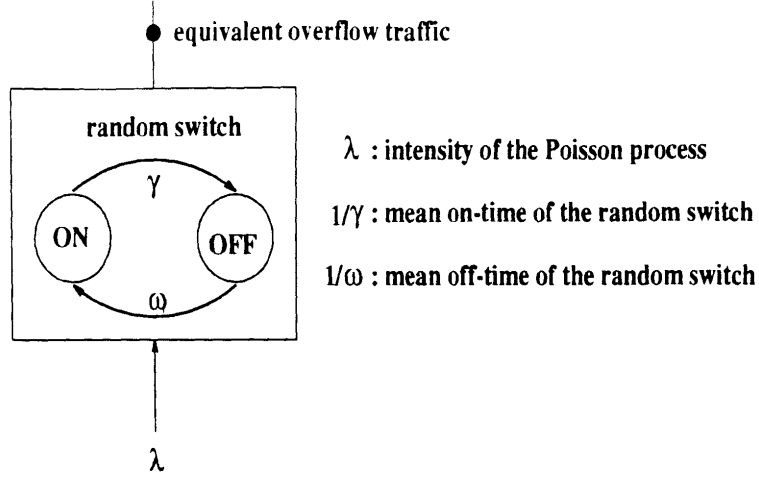


Figure 5: The conceptual structure of an *IPP* and its use for modeling overflow traffic.

resulting overflow traffic has the same mean, α_T , and variance, v_T . Following [12], given α_T and v_T , A and S can be determined as follows. First find

$$\begin{aligned} A' &= v_T + 3z(z - 1) \\ S' &= \frac{A(\alpha_T + z)}{\alpha_T + z - 1} - \alpha_T - 1, \end{aligned} \quad (14)$$

where z denotes the peakedness factor of the composite overflow traffic ($z = v_T/\alpha_T$). Then S is found by rounding S' down to its integral part, $[S']$. The corresponding value of A that produces the desired overflow traffic is

$$A = \frac{(S + \alpha_T + 1)(\alpha_T + z - 1)}{\alpha_T + z} \quad (15)$$

Once A and S are determined, the first three factorial moments of the composite overflow traffic, $M_{(i)}$, ($i = 1, 2, 3$), can be readily obtained by applying Kosten's moment formula [13]. That is,

$$M_{(n)} = A^n \frac{\sigma_0(S)}{\sigma_n(S)} \quad n = 1, 2, 3, \dots \quad (16)$$

in which

$$\sigma_0(S) = \frac{A^S}{S!}$$

and

$$\sigma_j(S) = \sum_{i=0}^S \binom{j+i-1}{i} \frac{A^{S-i}}{(S-i)!}, \quad j = 1, 2, 3, 4, \dots$$

Modified general formulas that determine three *IPP* parameters (i.e. λ , γ , and ω) to match the first three factorial moments of overflow traffic are derived in the Appendix of this paper, written as

$$\begin{aligned}\lambda &= \mu \cdot \frac{(2\delta_2 - \delta_1)(\delta_1 - \delta_0) - \delta_1(\delta_2 - \delta_1)}{(\delta_1 - \delta_0) - (\delta_2 - \delta_1)} \\ \omega &= \mu \cdot \frac{\delta_0 \left(\frac{\lambda}{\mu} - \delta_1\right)}{\frac{\lambda}{\mu} (\delta_1 - \delta_0)} \\ \gamma &= \omega \cdot \frac{\left(\frac{\lambda}{\mu} - \delta_0\right)}{\delta_0}\end{aligned}\tag{17}$$

where

$$\delta_n = \frac{M_{(n+1)}}{M_{(n)}},$$

and μ^{-1} is the mean holding time of channels in the overflow group to which the *IPP* is submitted, i.e. *unencumbered session duration*.

It has been rigorously shown in [9] that an *IPP* can accurately approximate overflow traffic. Intuitively, it is clear that for accurate modeling of overflow traffic the determined *IPP* parameters must generate a traffic stream (at least) whose *mean* is the same as that of composite overflow traffic, α_T . The mean of the load *submitted* by an *IPP* source is simply the mean of modulated Poisson process multiplying the probability of the random switch being *on*. That is,

$$\left(\frac{\lambda}{\mu}\right) \cdot \left(\frac{\omega}{\gamma + \omega}\right) \approx \alpha_T\tag{18}$$

in which the first factor on the left is the mean offered load of modulated Poisson process and the second factor on the left is the probability that the random switch is *on*.

IV.4 Macrocell Level

A macrocell under observation, after the composite overflow traffic is modeled by an *IPP*, has the input streams as depicted in Figure 6, in which X represents the random switch of determined *IPP*. When the random switch X is in the *on* state, arrivals of the offered overflow traffic follow a Poisson process with mean arrival rate λ . Each overflow arrival is an overflow due to new calls of high mobility type with probability p_1 , due to new calls of low mobility type with probability p_2 , due to hand-off calls of high mobility type with probability p_3 , and due to hand-off calls of low mobility type with probability p_4 . Specifically, when the random switch is in the *on* state, let A_{H1} , A_{L1} , A_{Hh1} , and A_{Lh1} denote the mean overflow traffic

arrival rates from subordinate microcells that represent new calls of high mobility type, new calls of low mobility type, hand-off calls of high mobility type, and hand-off calls of low mobility type, respectively. They can be written as

$$\begin{aligned}
A_{H1} &= \lambda \cdot p_1 = \lambda \cdot \frac{1}{\alpha_T} \left(\frac{\Lambda_{H1}}{\mu} P_{N1} N_1 \right) \\
A_{L1} &= \lambda \cdot p_2 = \lambda \cdot \frac{1}{\alpha_T} \left(\frac{\Lambda_{L1}}{\mu} P_{N1} N_1 \right) \\
A_{Hh1} &= \lambda \cdot p_3 = \lambda \cdot \frac{1}{\alpha_T} \left(\frac{\Lambda_{Hh1}}{\mu} P_{h1} N_1 \right) \\
A_{Lh1} &= \lambda \cdot p_4 = \lambda \cdot \frac{1}{\alpha_T} \left(\frac{\Lambda_{Lh1}}{\mu} P_{h1} N_1 \right)
\end{aligned} \tag{19}$$

Using Equ. (12), they can be rewritten in terms of *IPP* parameters as

$$\begin{aligned}
A_{H1} &\approx \frac{(\gamma + \omega)}{\omega} \cdot (\Lambda_{H1} P_{N1} N_1) \\
A_{L1} &\approx \frac{(\gamma + \omega)}{\omega} \cdot (\Lambda_{L1} P_{N1} N_1) \\
A_{Hh1} &\approx \frac{(\gamma + \omega)}{\omega} \cdot (\Lambda_{Hh1} P_{N1} N_1) \\
A_{Lh1} &\approx \frac{(\gamma + \omega)}{\omega} \cdot (\Lambda_{Lh1} P_{N1} N_1)
\end{aligned} \tag{20}$$

An overlaying macrocell of Figure 6 is described by the state (h, l, X) with equilibrium state probability $P_2(h, l, X)$, in which h and l is the number of communicating high- and low mobility platforms in the observed macrocell, respectively, and X is the state of *IPP* random switch taking the value of 1 if the process is *on*, of 0 if the process is *off*. System equations can be formulated in a way similar to that used in the analysis of a microcell. Let

$$\phi_{n2} = \begin{cases} 0 & \text{if } (h + l) = C_2 - C_{h2}, \\ 1 & \text{otherwise.} \end{cases} \tag{21}$$

$$\phi_{h2} = \begin{cases} 0 & \text{if } (h + l) = C_2, \\ 1 & \text{otherwise.} \end{cases} \tag{22}$$

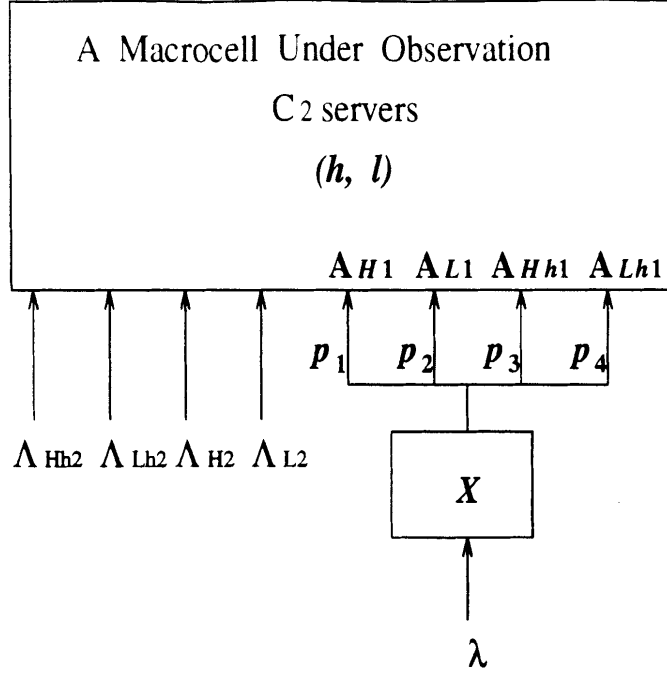


Figure 6: Analysis of an overlaying macrocell under observation.

Then, the equilibrium state equations for $0 \leq (h + l) \leq (C_2 - C_{h2})$ are given by

$$\begin{aligned}
 & (\Lambda_{H2}\phi_{n2} + \Lambda_{L2}\phi_{n2} + \Lambda_{Hh2} + \Lambda_{Lh2} + (h + l)\mu + hU_{HD2} + lU_{LD2} + \omega)P_2(h, l, 0) \\
 & = \gamma P_2(h, l, 1) + (\Lambda_{H2} + \Lambda_{Hh2})P_2(h - 1, l, 0) + (\Lambda_{L2} + \Lambda_{Lh2})P_2(h, l - 1, 0) \\
 & + [(h + 1)\mu + (h + 1)U_{HD2}]P_2(h + 1, l, 0) + [(l + 1)\mu + (l + 1)U_{LD2}]P_2(h, l + 1, 0) \\
 & [P_2(-1, l, 0) = P_2(h, -1, 0) = 0]
 \end{aligned} \tag{23}$$

$$\begin{aligned}
 & [(\Lambda_{H2} + \Lambda_{L2} + A_{H1} + A_{L1})\phi_{n2} + \Lambda_{Hh2} + \Lambda_{Lh2} + A_{Hh1} + A_{Lh1} \\
 & + (h + 1)\mu + hU_{HD2} + lU_{LD2} + \gamma]P_2(h, l, 1) \\
 & = \omega P_2(h, l, 0) + (\Lambda_{H2} + \Lambda_{Hh2} + A_{H1} + A_{Hh1})P_2(h - 1, l, 1) \\
 & + (\Lambda_{L2} + \Lambda_{Lh2} + A_{L1} + A_{Lh1})P_2(h, l - 1, 1) \\
 & + [(h + 1)\mu + (h + 1)U_{HD2}]P_2(h + 1, l, 1) \\
 & + [(l + 1)\mu + (l + 1)U_{LD2}]P_2(h, l + 1, 1) \\
 & [P_2(-1, l, 0) = P_2(h, -1, 0) = 0]
 \end{aligned} \tag{24}$$

For $(C_2 - C_{h_2}) < (h + l) \leq C_2$, they are written as

$$\begin{aligned}
& [(\Lambda_{Hh_2} + \Lambda_{Lh_2})\phi_{h_2} + (h + l)\mu + hU_{HD2} + lU_{LD2} + \omega]P_2(h, l, 0) \\
& = \gamma P_2(h, l, 1) + \Lambda_{Hh_2}P_2(h - 1, l, 0) + \Lambda_{Lh_2}P_2(h, l - 1, 0) \\
& + [(h + 1)\mu + (h + 1)U_{HD2}]P_2(h + 1, l, 0) + [(l + 1)\mu + (l + 1)U_{LD2}]P_2(h, l + 1, 0) \\
& [P_2(h, l, X)|_{(h+l)>C_2} = 0]
\end{aligned} \tag{25}$$

$$\begin{aligned}
& [(\Lambda_{Hh_2} + \Lambda_{Lh_2} + A_{Hh_1} + A_{Lh_1})\phi_{h_2} + (h + l)\mu + hU_{HD2} + lU_{LD2} + \gamma]P_2(h, l, 1) \\
& = \omega P_2(h, l, 0) + (\Lambda_{Hh_2} + A_{Hh_1})P_2(h - 1, l, 1) + (\Lambda_{Lh_2} + A_{Lh_1})P_2(h, l - 1, 1) \\
& + [(h + 1)\mu + (h + 1)U_{HD2}]P_2(h + 1, l, 1) + [(l + 1)\mu + (l + 1)U_{LD2}]P_2(h, l + 1, 1) \\
& [P_2(h, l, X)|_{(h+l)>C_2} = 0]
\end{aligned} \tag{26}$$

An example macrocell state-transition diagram for the case $C_2 = 4$, $C_{h_2} = 1$ is shown in Figure 7. State equations can be solved for state probabilities, subject to the normalization equations

$$\Pr\{\text{switch is on}\} = \sum_{h=0}^{C_2} \sum_{l=0}^{C_2} P_2(h, l, 1) = \frac{\frac{1}{\gamma}}{\frac{1}{\gamma} + \frac{1}{\omega}} = \frac{\omega}{\gamma + \omega} \tag{27}$$

and

$$\Pr\{\text{switch is off}\} = \sum_{h=0}^{C_2} \sum_{l=0}^{C_2} P_2(h, l, 0) = \frac{\frac{1}{\omega}}{\frac{1}{\gamma} + \frac{1}{\omega}} = \frac{\gamma}{\gamma + \omega} . \tag{28}$$

Once macrocell state probabilities are determined, the probability that a new call is denied access to a macrocell channel and hence overflowed to its overlaying spot beam, P_{N_2} , is given by

$$P_{N_2} = \sum_{(h+l)=C_2-C_{h_2}}^{C_2} [P_2(h, l, 0) + P_2(h, l, 1)] , \tag{29}$$

and the *conditional* probability that the macrocell will not be able to serve a new call when an overflowed new call arrives is

$$P_{B_2} = \sum_{(h+l)=C_2-C_{h_2}}^{C_2} P_2(h, l, 1) . \tag{30}$$

The probability that a hand-off call finds all channels in a macrocell occupied upon arrival and is hence overflowed to the overlaying spot beam, P_{h_2} , is therefore

$$P_{h_2} = \sum_{(h+l)=C_2} (P_2(h, l, 0) + P_2(h, l, 1)) . \tag{31}$$

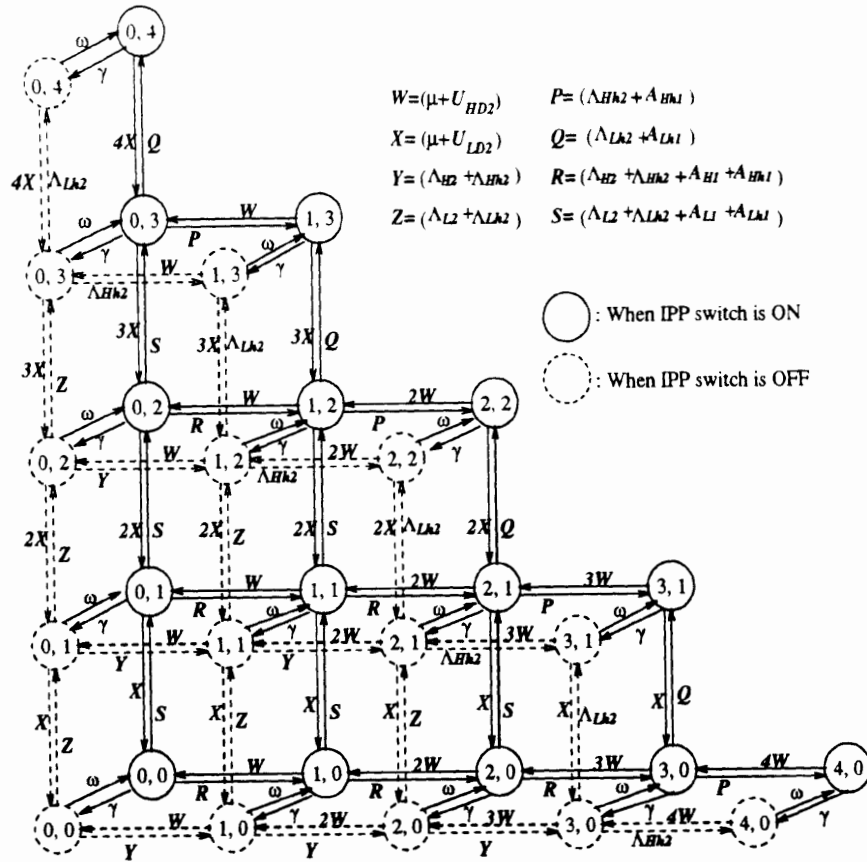


Figure 7: An example state-transition diagram for the analysis of a macrocell whose $C_2 = 4$ and $C_{h2} = 1$.

Analysis of the spot beam level follows an approach similar to that used for macrocells, except that the *overflowed new calls* will be accommodated only when the number of channels in use is less than $C_3 - C_{h3} - C_s$, but the *primary new calls* can access up to $C_3 - C_{h3}$ channels. Therefore, the blocking probability for *primary new calls*, P_{N3} , is written as

$$P_{N3} = \sum_{(h+l)=C_3-C_{h3}}^{C_3} (P_3(h, l, 0) + P_3(h, l, 1)) , \quad (32)$$

and the *conditional* probability that the spot beam would not be able to serve a new call when an overflowed new call arrives is

$$P_{B3} = \sum_{(h+l)=C_3-C_{h3}-C_s}^{C_3} P_3(h, l, 1) , \quad (33)$$

The probability that a hand-off call finds all channels in a spot beam occupied upon arrival and is hence *forced to terminate*, P_{h3} , is

$$P_{h3} = \sum_{(h+l)=C_3} \sum (P_3(h, l, 0) + P_3(h, l, 1)) . \quad (34)$$

Overall system performance can be derived once each system level is analyzed.

V Performance Measures

V.1 Blocking Probability

The blocking probability is the probability that *new call* arrivals are denied access to a channel. Blocking events occur when the channels (that are accessible by new calls) in the initially attempted cell as well as overlaying cells are all occupied *and* a new call arrives. The probability that a microcell and a macrocell can not serve a new call is P_{N1} and P_{N2} , respectively. The *conditional* probability that the overlaying macrocell can not serve a new call given that an overflowed new call arrives is P_{B2} , and that conditional probability for overlaying spot beam is P_{B3} . Thus the overall blocking probability for a new call attempt that is initially directed to the preferred microcell is given by $P_{N1}P_{B2}P_{B3}$. Similarly, the overall blocking probability for a new call attempt that is initially directed to the preferred macrocell is $P_{N2}P_{B3}$. For new call attempts that are initially directed to the overlaying spot beam, the overall blocking probability is simply P_{N3} . Recall that a new call may be directed by the system to look for idle channels starting from the i_{th} level with probabilities f_i . The overall blocking probability, P_B , for a new call origination in the system is written as

$$P_B = f_1 P_{N1} P_{B2} P_{B3} + f_2 P_{N2} P_{B3} + f_3 P_{N3} \quad (35)$$

Note that new calls originated from high mobility platforms will experience the same blocking probability as those from low mobility platforms. For satellite-only subscribers, the blocking probability is simply P_{N3} .

V.2 Forced Termination Probability

The forced termination probability, P_{FT} , is the probability that a call which is not initially blocked is interrupted *due to hand-off failure* during its lifetime. We start formulating the

forced termination probability by considering the initial cell assignment of an *accommodated* new call. The derivation presented here is in terms of high mobility platforms but the same arguments are applicable for low mobility platforms as well.

Given that a new call origination is accommodated by the system, the probability that this new call is accommodated by the i_{th} hierarchical cell is denoted as S_i . The probability that a new call origination will be *accommodated by the system* is $1 - P_B$, of which the probability that a new call origination will be *served by a microcell* is $f_1(1 - P_{N1})$, *by a macrocell* with probability $f_1 P_{N1}(1 - P_{B2}) + f_2(1 - P_{N2})$, and *by a spot beam* with probability $f_1 P_{N1} P_{B2}(1 - P_{B3}) + f_2 P_{N2}(1 - P_{B3}) + f_3(1 - P_{N3})$. Therefore, S_i ($i = 1, 2, 3$) can be written as

$$\begin{aligned} S_1 &= \frac{f_1(1 - P_{N1})}{1 - P_B} \\ S_2 &= \frac{f_1 P_{N1}(1 - P_{B2}) + f_2(1 - P_{N2})}{1 - P_B} \\ S_3 &= \frac{f_1 P_{N1} P_{B2}(1 - P_{B3}) + f_2 P_{N2}(1 - P_{B3}) + f_3(1 - P_{N3})}{1 - P_B} \end{aligned}$$

Note that $S_1 + S_2 + S_3 = 1$.

Now, consider a call of high mobility type that is in progress in a cell of level i . The probability that a high mobility call currently served by a cell of level i will make another hand-off attempt *and* be successfully accommodated by neighboring cells of the *same level*, a_i , is found to be

$$a_i = \frac{U_{HDi}}{\mu + U_{HDi}} \cdot (1 - P_{hi}) \quad (36)$$

The probability that a high mobility call currently served by a cell of level i will make another hand-off attempt *and* be denied access to a channel of level i (thus is overflowed to next higher level or forced into termination), b_i , is given by

$$b_i = \frac{U_{HDi}}{\mu + U_{HDi}} \cdot P_{hi} \quad (37)$$

With independent hand-off attempts, the probability that a high mobility call currently served by a cell of level i will **exit** from the i_{th} level, E_i , is given as

$$E_i = b_i + a_i b_i + a_i^2 b_i + \dots = \frac{U_{HDi} P_{hi}}{\mu + U_{HDi} P_{hi}} \quad (38)$$

Now let us focus attention on a new call that is initially accommodated by the first level, a microcell. When this call *exits* from the service of the first level, it might be handed off

to the second, to the third level or simply forced into termination immediately. Taking all situations into account, the forced termination probability for a call that is initially served by a microcell, P_{FT1} , can be written as

$$\begin{aligned}
& S_1 E_1 (1 - P_{h2}) E_2 (1 - P_{h3}) E_3 && 1 \rightarrow 2 \rightarrow 3 \Rightarrow \text{forced term.} \\
& + S_1 E_1 (1 - P_{h2}) E_2 P_{h3} && 1 \rightarrow 2 \Rightarrow \text{forced term.} \\
& + S_1 E_1 P_{h2} (1 - P_{h3}) E_3 && 1 \rightarrow 3 \Rightarrow \text{forced term.} \\
& + S_1 E_1 P_{h2} P_{h3} && 1 \Rightarrow \text{forced term.}
\end{aligned} \tag{39}$$

where the first term accounts for the probability that a call which is initially served by a microcell will exit from the service of the microcell level, get accommodated by the macrocell level, exit from the macrocell level, get accommodated by the overlaying spot beam level, exit again from the overlaying spot beam and be forced into termination. The right side of the first term indicates the transition of system levels with forced termination abbreviated as *forced term..*

For calls initially served by the second level, macrocell, the forced termination probability, P_{FT2} , is

$$\begin{aligned}
& S_2 E_2 (1 - P_{h3}) E_3 && 2 \rightarrow 3 \Rightarrow \text{forced term.} \\
& + S_2 E_2 P_{h3} && 2 \Rightarrow \text{forced term.}
\end{aligned} \tag{40}$$

Using these results we find the following expression for the forced termination probability (including forced terminations for calls initially served at level 3):

$$P_{FT} = P_{FT1} + P_{FT2} + S_3 E_3 \tag{41}$$

V.3 Traffic Distribution and Carried Traffic

Given the equilibrium state probabilities of each level, traffic distributions and traffic carried by the system can be readily determined. Let $V_i(H)$ and $V_i(L)$ denote the high mobility and low mobility traffic carried by the i_{th} system level, respectively. Then,

$$V_i(H) = \sum_{h=0}^{C_i} \sum_{l=0}^{C_i} h \cdot P_i(h, l) \tag{42}$$

$$V_i(L) = \sum_{h=0}^{C_i} \sum_{l=0}^{C_i} l \cdot P_i(h, l), \tag{43}$$

in which $P_i(h, l) = P_i(h, l, 0) + P_i(h, l, 1)$ for $i = 2, 3$.

The total traffic carried by the system, A_c , is thus

$$A_c = \sum_{i=1}^3 V_i(H) + V_i(L) \tag{44}$$

VI Examples and Discussions

A three-level hierarchically overlaid system as depicted in Figure 1 is considered as a numerical example to illustrate the performance analysis techniques presented here. Each microcell region is randomly traversed by 100 *dual users* that are of high mobility and another 100 of low mobility type. The number of *satellite-only users* in each spot beam region is 80 for each mobility type. The new call origination rate from noncommunicating platforms, regardless of the platform mobility and service subscribed, was varied from 4.5×10^{-4} to 5.5×10^{-4} calls/sec. The mean unencumbered call duration is 100 sec. The dwell time of high mobility platforms in a microcell, macrocell, and spot beam are initially taken as 50 sec, 185 sec, and 500 sec, respectively. The dwell time of low mobility platforms is 5 times longer than that of high mobility platforms at each system level. The number of channels allocated to each microcell, macrocell, and spot beam are 10, 18, and 70, respectively, of which only one channel in each cell is reserved for the exclusive use of hand-off calls. That is, $C_1 = 10$, $C_2 = 18$, $C_3 = 70$, and $C_{hi} = 1$ for $i = 1, 2, 3$. With $C_s = 3$ in this example, a spot beam will accommodate an *overflowed new call* only if the number of channels in use is less than 66, and will accommodate a *primary new call* if the number of channels in use is less than 69. Each new call origination from a *dual user* will be directed to a microcell with probability 0.93, to a macrocell with probability 0.05, and to a spot beam with probability 0.02.

Figure 8 shows the blocking and forced termination probabilities for dual users and satellite-only users. It can be seen that the multi-layer hierarchically overlaid system has excellent performance from low to moderate load, but degrades sharply and levels off when the offered load becomes too large. This is because the use of 70 channels in a spot beam to overlay 49 microcells renders insufficient overlay in high traffic demand. The use of overlay channels is cost-effective since it provides not only enhanced performance till moderate load, but also graceful degradation in high traffic demand. High mobility platforms are seen to experience a higher forced termination probability, P_{FT} , than low mobility platforms. Since *satellite-only users* have much longer dwell time than dual users, they experience lower P_{FT} over a wide range of offered load than dual users, even though the dual users potentially have more accessible channels.

Figure 9 shows the teletraffic carried by each level and Figure 10 shows the fraction of carried traffic that is of high- and low mobility types. The traffic carried by a *spot beam* is seen to increase significantly when the offered load is increased. That is, channels of a

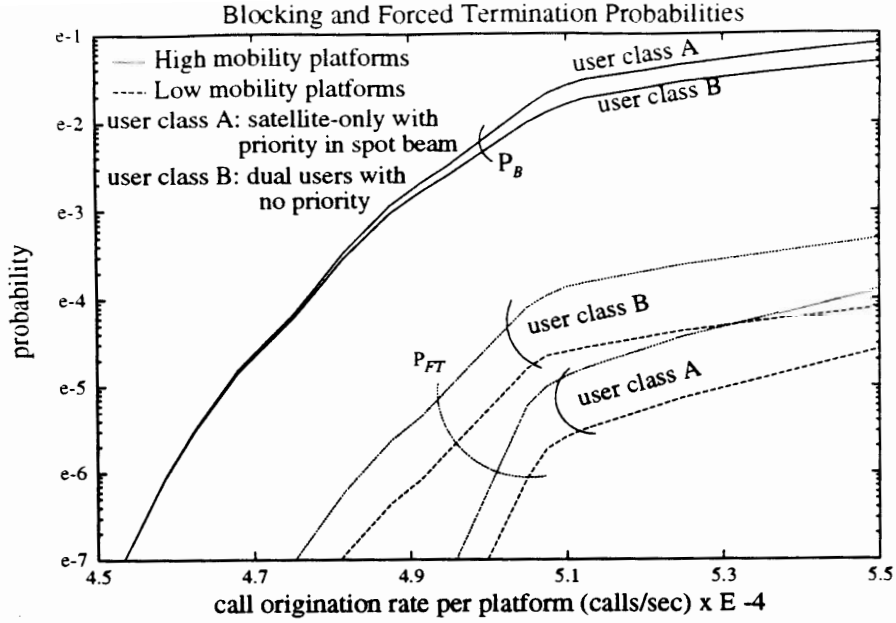


Figure 8: Blocking and forced termination probabilities depend on call demand. The dwell times are $\bar{T}_{HD1} = 50$ sec, $\bar{T}_{HD2} = 185$ sec, $\bar{T}_{HD3} = 500$ sec, and $\bar{T}_{LDi} = 5 \cdot \bar{T}_{HDi}$ for $i = 1, 2, 3$.

spot beam normally remain unused unless no channels in lower levels are available to serve a call. The traffic distribution in Figure 10 shows that most of the traffic carried by a spot beam are of high mobility type, whereas microcell channels are predominately occupied by low mobility platforms. As offered traffic increases, the capability of such an autonomous mobility management becomes more apparent.

Let the system be operated at an origination rate of 5.05×10^{-4} calls/sec/platform. How the platform mobility (i.e. dwell time) affect system performance is of interest. The dwell times set forth earlier are defined as the *reference dwell time*. Dwell time now is varied from 0.7 times the reference dwell time to 1.5 times the reference value. The impact of dwell time variation on blocking and forced termination probabilities is shown on Figure 11. From Figure 11, the platform speed (dwell time) has a much more significant impact on P_{FT} than on P_B . As the platform dwell time decreases, more frequent hand-offs can be expected during the lifetime of a call; therefore, P_{FT} increases. As a result of using multiple overlays, P_{FT} degrades gracefully. The variation of dwell times cause no significant change in carried traffic, as shown in Figure 12. Figure 13 demonstrates that our system has inherent mobility

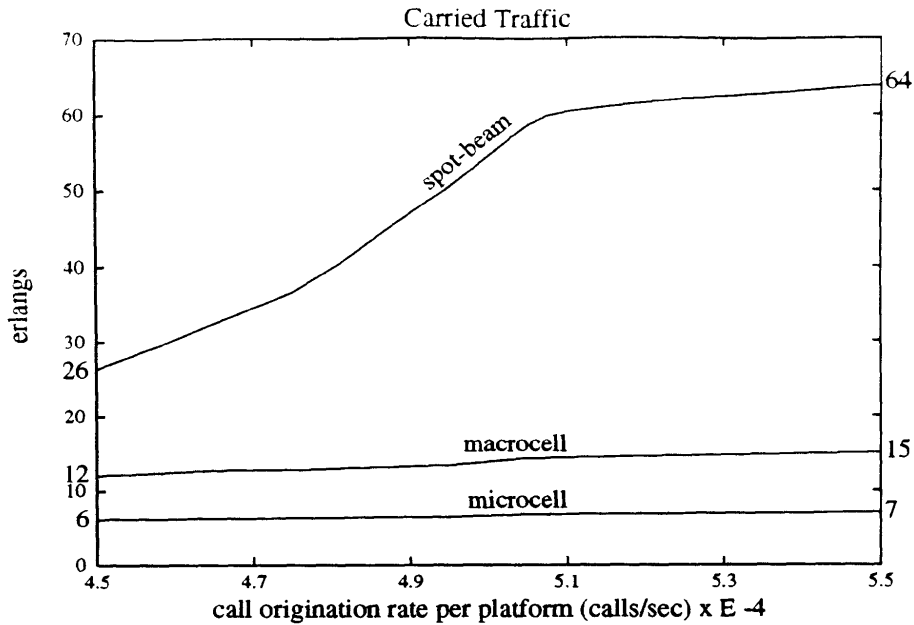


Figure 9: Teletraffic carried by single cell at different hierarchical levels.

management capability. It can be seen that a higher percentage of spot beam channels are used by high mobility platforms when their dwell times are decreased.

VII Conclusions

A personal communication system with multiple hierarchical cellular overlays is considered. Users are classified into *dual users* and *satellite-only users*, whereas the platforms are classified into *high mobility* and *low mobility* types. Hand-offs are given priority access to channels. Analytical method for analyzing the performance (including hand-off) of such a multi-layer hierarchical overflow system is developed. Theoretical performance characteristics for users having different mobilities are calculated. With the use of multiple hierarchical overlays, system performance is enhanced. The resultant system is robust with wide coverage areas, high channel capacity, and has inherent load-balancing and mobility-management capabilities.

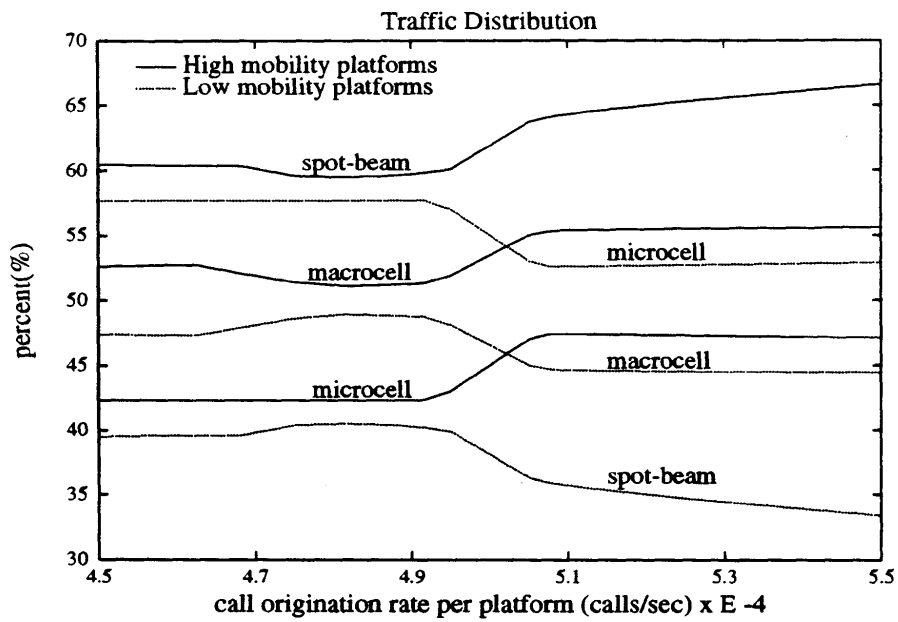


Figure 10: Distribution of platform types served at different hierarchical levels.

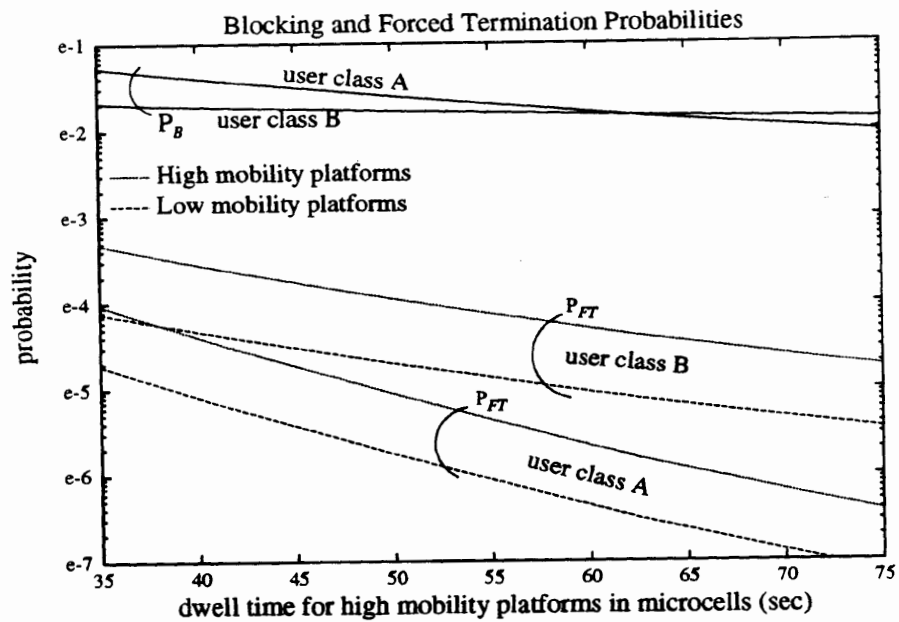


Figure 11: Blocking and forced termination probabilities depend on dwell times. System is operated at a call origination rate of 5.05×10^{-4} calls/sec per platform. Dwell times for low mobility platforms in various hierarchical levels are scaled in proportion to that of \bar{T}_{HD1} .

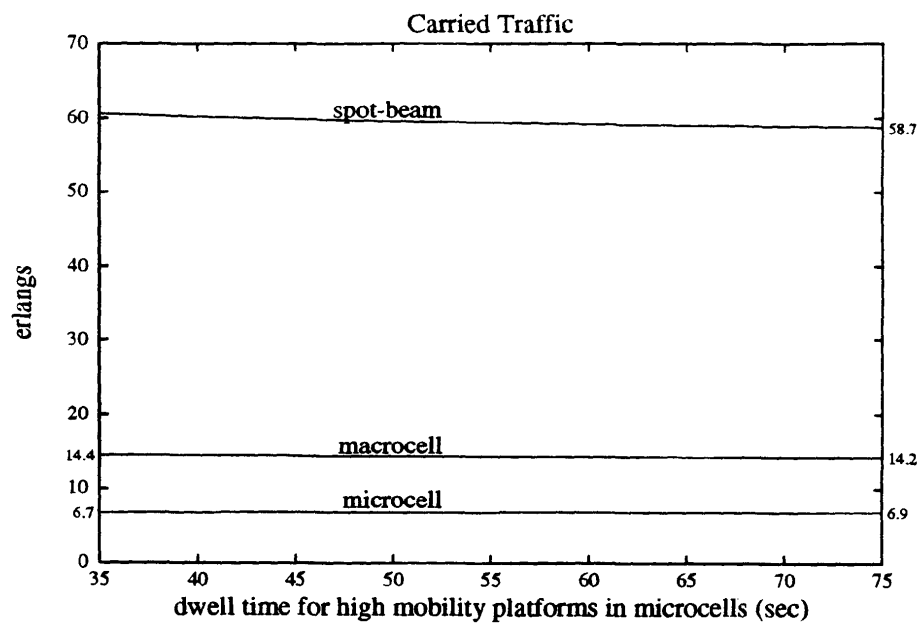


Figure 12: Teletraffic carried by single cell at different hierarchical levels depend on dwell times.

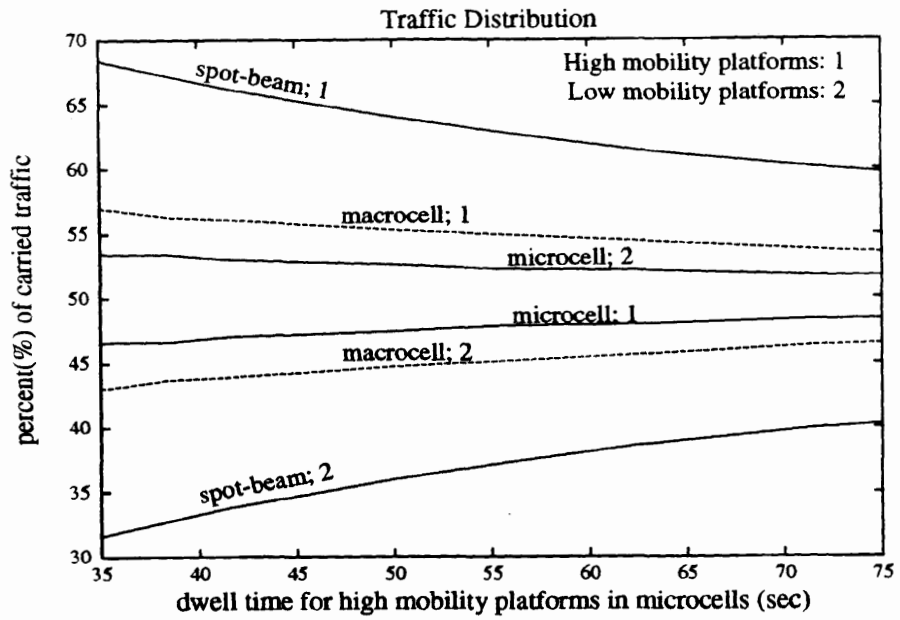


Figure 13: Distributions of platform types served at different hierarchical level depend on dwell times.

References

- [1] S. S. Rappaport and L-R. Hu. "Microcellular Communication Systems with Hierarchical Macrocell Overlays: Traffic Performance Models and Analysis," *Proceedings of the IEEE*, vol. 82, pp. 1383-1397, Sept. 1994.
- [2] M. Carosi and B. Pavesi *et. al*, "A Suitable Architecture For Personal Communications Systems Based on Small Satellites," in *Proc. IEEE Int'l Conf. on Universal Personal Comm.*, ICUPC 1993, pp. 284-290.
- [3] M. Horstein, "ODYSSEY - A Satellite-Based Personal Communication System," in *Proc. IEEE Int'l Conf. on Universal Personal Comm.*, ICUPC 1993, pp. 291-298.
- [4] T. Kipreos, "Satellites and PCS : The Hybrid Approach," in *Proc. IEEE Int'l Conf. on Universal Personal Comm.*, ICUPC 1993, pp. 334-338.
- [5] R. Steele and M. Nofal, "Teletraffic Performance of Microcellular Personal Communication Networks," *IEE Proceedings-I*, vol. 139, pp. 448-461, Aug. 1992.
- [6] H. Eriksson and B. Gudmundson *et. al*, "Multiple Access Options for Cellular Based Personal Communications," in *Proc. IEEE Veh. Technol. Conf.*, VTC 1993, pp. 957-962.
- [7] C-L. I, L. J. Greenstein, and R. D. Gitlin, "A Microcell/Macrocell Cellular Architecture for Low- and High-Mobility Wireless Users," *IEEE J. Selected Areas in Commun.*, vol. 11, pp. 885-891, Aug. 1993.
- [8] L-P. Chin and J-F. Chang, "Performance Analysis of a Hierarchical Cellular Mobile Communication System," in *Proc. IEEE Int'l Conf. on Universal Personal Comm.*, ICUPC 1993, pp. 128-132.
- [9] A. Kuczura, "The Interrupted Poisson Process As An Overflow Process," *Bell Syst. Tech. J.*, vol. 52, pp. 437-448, March 1973.
- [10] S. S. Rappaport, "The multiple-call hand-off problem in high-capacity cellular communications systems," *IEEE Trans. Veh. Technol.*, vol. VT-40, pp. 546-557, Aug. 1991.
- [11] S. S. Rappaport, "Blocking, hand-off and traffic performance for cellular communication systems with mixed platforms," *IEE(British) Proceedings*, Part I, vol. 140, pp. 389-401, Oct. 1993.
- [12] R. B. Cooper, *Introduction to Queueing Theory*, 3rd ed., Washington D.C., CeePress, 1990.
- [13] R. I. Wilkinson, "Theories for Toll Traffic Engineering in the U.S.A.," with Appendix by J. Riordan, "Derivation of Moments of Overflow Traffic," *Bell Syst. Tech. J.*, vol. 35, pp. 421-514, March 1956.
- [14] V. S. Frost and B. Melamed, "Traffic Modeling for Telecommunications Networks," *IEEE Communications Magazine*, pp. 70-81, March 1994.

Appendix

Derivation of Moment-Match Equations for IPP Parameters

The derivation here is based on fundamental principles that if an *interrupted Poisson process* (IPP) is to model an overflow traffic, characterized by the first three factorial moments, it must generate the same amounts of moments in an infinite trunk group. Following the derivation in [9], let an IPP be offered to an infinite trunk group. Let λ be the intensity of the Poisson process, $1/\gamma$ be the mean on-time of the random switch, $1/\omega$ be the mean off-time, and $1/\mu$ be the mean channel holding time. The state of the system is described by (m, n) where m is the number of channels busy in the infinite trunk group, and n is the state of the random switch taking the value of “1” when the switch is “on”, or the value of “0” when the switch is “off”. The equilibrium equations for the stationary state probabilities, $p(m, n)$, are

$$\begin{aligned}
 (m\mu + \omega)p(m, 0) &= \gamma p(m, 1) + (m + 1)\mu p(m + 1, 0) \quad m \geq 0, \\
 (m\mu + \gamma + \lambda)p(m, 1) &= \omega p(m, 0) + (m + 1)\mu p(m + 1, 1) + \lambda p(m - 1, 1), \\
 &\quad m \geq 1, \\
 (\gamma + \lambda)p(0, 1) &= \omega p(0, 0) + \mu p(1, 1).
 \end{aligned} \tag{1}$$

The normalization equations for IPP-driven system are

$$\text{Pr.}\{\text{switch is ON}\} = \sum_{m=0}^{\infty} p(m, 1) = \frac{\frac{1}{\gamma}}{\frac{1}{\gamma} + \frac{1}{\omega}} = \frac{\omega}{\gamma + \omega} \tag{2}$$

and

$$\text{Pr.}\{\text{switch is OFF}\} = \sum_{m=0}^{\infty} p(m, 0) = \frac{\frac{1}{\omega}}{\frac{1}{\gamma} + \frac{1}{\omega}} = \frac{\gamma}{\gamma + \omega} \tag{3}$$

This system of equations is solved by [9], using probability generating function

$$G(z) = \sum_{m=0}^{\infty} [p(m, 0) + p(m, 1)]z^m \tag{4}$$

The obtained solution is

$$G(z) = \frac{\gamma}{\gamma + \omega} F\left[\beta, \epsilon, \frac{\lambda}{\mu}(z - 1)\right] + \frac{\omega}{\gamma + \omega} F\left[1 + \beta, \epsilon, \frac{\lambda}{\mu}(z - 1)\right], \tag{5}$$

where

$$\beta = \frac{\omega}{\mu}, \quad \epsilon = 1 + \frac{\gamma + \omega}{\mu}, \tag{6}$$

and¹

$$F[a, b, c] = \sum_{n=0}^{\infty} \frac{(a)_n c^n}{(b)_n} \quad (7)$$

with

$$(a)_n = a(a+1)(a+2)\dots(a+n-1), \quad (a)_0 = 1. \quad (8)$$

The factorial moments of the distribution of the number of busy channels in the infinite trunk group are the coefficients of power series expansion on Equation (5) about $z = 1$. Let $G^n(1)$ denote the n_{th} factorial moment. Then, we obtain

$$\begin{aligned} G^1(1) &= \frac{\frac{\lambda}{\mu} \cdot \omega}{\gamma + \omega} \\ G^2(1) &= \frac{\left(\frac{\lambda}{\mu}\right)^2 \cdot \omega(\omega + \mu)}{(\gamma + \omega)(\gamma + \omega + \mu)} \\ G^3(1) &= \frac{\left(\frac{\lambda}{\mu}\right)^3 \cdot \omega(\omega + \mu)(\omega + 2\mu)}{(\gamma + \omega)(\gamma + \omega + \mu)(\gamma + \omega + 2\mu)} \end{aligned} \quad (9)$$

Now, let $M_{(n)}$ be the n_{th} factorial moment of overflow traffic and

$$\delta_n = \frac{M_{(n+1)}}{M_{(n)}}.$$

By matching the first three factorial moments, that is,

$$G^n(1) = M_{(n)}, \quad n = 1, 2, 3, \quad (10)$$

we obtain

$$\frac{\lambda}{\mu} \omega = \delta_0(\gamma + \omega) \quad (11)$$

$$\frac{\lambda}{\mu}(\omega + \mu) = \delta_1(\gamma + \omega + \mu) \quad (12)$$

$$\frac{\lambda}{\mu}(\omega + 2\mu) = \delta_2(\gamma + \omega + 2\mu) \quad (13)$$

Subtract (11) from (12),

$$\begin{aligned} \lambda &= \delta_1(\gamma + \omega + \mu) - \delta_0(\gamma + \omega) \\ &= (\gamma + \omega)(\delta_1 - \delta_0) + \delta_1\mu \end{aligned}$$

Thus

$$\Rightarrow (\lambda - \delta_1\mu) = (\gamma + \omega)(\delta_1 - \delta_0) \quad (14)$$

¹The original manuscript had a redundant term, $n!$, in the denominator of $F[a, b, c]$

Similarly, by subtracting (12) from (13),

$$\begin{aligned}\lambda &= \delta_2(\gamma + \omega + 2\mu) - \delta_1(\gamma + \omega + \mu) \\ &= (\gamma + \omega)(\delta_2 - \delta_1) + (2\mu\delta_2 - \mu\delta_1)\end{aligned}$$

Thus

$$\Rightarrow \lambda - (2\mu\delta_2 - \mu\delta_1) = (\gamma + \omega)(\delta_2 - \delta_1) \quad (15)$$

Dividing (14) by (15), we obtain

$$\frac{\lambda - \delta_1\mu}{\lambda - (2\mu\delta_2 - \mu\delta_1)} = \frac{\delta_1 - \delta_0}{\delta_2 - \delta_1} \quad (16)$$

Cross-multiply (16) and rearrange the terms

$$\begin{aligned}\Rightarrow \lambda(\delta_2 - \delta_1) - \delta_1\mu(\delta_2 - \delta_1) &= \lambda(\delta_1 - \delta_0) - (2\mu\delta_2 - \mu\delta_1)(\delta_1 - \delta_0) \\ \Rightarrow \lambda[(\delta_1 - \delta_0) - (\delta_2 - \delta_1)] &= (2\mu\delta_2 - \mu\delta_1)(\delta_1 - \delta_0) - \delta_1\mu(\delta_2 - \delta_1)\end{aligned}$$

Therefore,

$$\lambda = \mu \cdot \frac{(2\delta_2 - \delta_1)(\delta_1 - \delta_0) - \delta_1(\delta_2 - \delta_1)}{(\delta_1 - \delta_0) - (\delta_2 - \delta_1)} \quad (17)$$

From (11),

$$\Rightarrow \lambda\omega = \delta_0\mu(\gamma + \omega) = \delta_0\mu\gamma + \delta_0\mu\omega \quad (18)$$

$$\Rightarrow (\lambda - \delta_0\mu)\omega = \delta_0\mu\gamma \quad (19)$$

Thus

$$\gamma = \omega \cdot \frac{(\lambda - \delta_0\mu)}{\delta_0\mu} = \omega \cdot \frac{(\frac{\lambda}{\mu} - \delta_0)}{\delta_0} \quad (20)$$

Substitute (11) into (12),

$$\begin{aligned}\Rightarrow \delta_0(\gamma + \omega) + \lambda &= \delta_1(\gamma + \omega + \mu) \\ \Rightarrow \gamma(\delta_0 - \delta_1) &= \omega(\delta_1 - \delta_0) + \delta_1\mu - \lambda \\ \Rightarrow \gamma &= -\omega + \frac{\delta_1\mu - \lambda}{\delta_0 - \delta_1}\end{aligned} \quad (21)$$

Equating (20) and (21), we obtain

$$\gamma = \omega \cdot \frac{(\lambda - \delta_0\mu)}{\delta_0\mu} = -\omega + \frac{\delta_1\mu - \lambda}{\delta_0 - \delta_1} \quad (22)$$

Rearrange the terms, we obtain the expression of ω .

$$\begin{aligned}
\Rightarrow \omega \left(\frac{\lambda}{\delta_0 \mu} - 1 \right) + \omega &= \frac{\delta_1 \mu - \lambda}{\delta_0 - \delta_1} \\
\Rightarrow \omega \cdot \frac{\lambda}{\delta_0 \mu} &= \frac{\delta_1 \mu - \lambda}{\delta_0 - \delta_1} \\
\Rightarrow \omega &= \frac{\delta_0 \mu}{\lambda} \cdot \frac{\delta_1 \mu - \lambda}{\delta_0 - \delta_1} \\
\Rightarrow \omega &= \frac{\delta_0}{\frac{\lambda}{\mu}} \cdot \frac{\mu(\delta_1 - \frac{\lambda}{\mu})}{(\delta_0 - \delta_1)} \tag{23}
\end{aligned}$$

Finally,

$$\omega = \mu \frac{\delta_0 \left(\frac{\lambda}{\mu} - \delta_1 \right)}{\frac{\lambda}{\mu} (\delta_1 - \delta_0)} \tag{24}$$

Summarizing (17), (20), and (24), the moment-match equations for IPP parameters are

$$\begin{aligned}
\lambda &= \mu \cdot \frac{(2\delta_2 - \delta_1)(\delta_1 - \delta_0) - \delta_1(\delta_2 - \delta_1)}{(\delta_1 - \delta_0) - (\delta_2 - \delta_1)} \\
\omega &= \mu \cdot \frac{\delta_0 \left(\frac{\lambda}{\mu} - \delta_1 \right)}{\frac{\lambda}{\mu} (\delta_1 - \delta_0)} \\
\gamma &= \omega \cdot \frac{\left(\frac{\lambda}{\mu} - \delta_0 \right)}{\delta_0} \tag{25}
\end{aligned}$$